CHEMICAL ENGINEERING TRANSACTIONS
VOL. 113, 2024
A publication of AIDIC
The Italian Association of Chemical Engineering
Online at www.cetjournal.it
Guest Editors: Jeng Shiun Lim, Bohong Wang, Guo Ren Mong, Petar S. Varbanov

ISBN 979-12-81206-14-4; **ISSN** 2283-9216
DOI: 10.3303/CET24113030

Effect of Air Preheating on the NO_X Emissions and Reaction Kinetics of Ammonia/Methane Flames under Different Fuel Injection Strategies

Siqi Wang[a], Cheng Tung Chong[a,*], Meng-Choung Chiong[b]

[a]China-UK Low Carbon College, Shanghai Jiao Tong University, Lingang, Shanghai, 201306, China
[b]Department of Mechanical Engineering, Faculty of Engineering, Technology, and Built Environment, UCSI University 56000 Kuala Lumpur, Malaysia.
ctchong@sjtu.edu.cn

With the rapid advancement of industrialization, the escalating demand for energy and need for decarbonization prompt for the development of alternative renewable energy sources and highly efficient, clean combustion technologies. Ammonia, being a carbon-free fuel and an excellent hydrogen carrier has gained widespread attention. However, challenges persist in using ammonia as a fuel include high NO_x pollutant emissions and the weak reactivity of ammonia. In this study, a swirl experimental platform was employed to investigate the effect of main air preheating on the flame and NO_x emissions characteristics of ammonia-methane. Two fuel injection strategies were compared, i.e., dual-fuel injection and premixed injection mode, to form a dual flame and fully premixed swirl flame. The chemiluminescence experiments were performed to analyse the intensities of OH^* emissions from flame. Numerical simulations were carried out using the chemical reaction network model. Results shows that both type of flames exhibit different flame structure, with dual flame exhibit higher OH^* chemiluminescence intensities. Comparing fully premixed combustion with dual flame combustion modes at T = 473 K and ϕ = 0.6, the latter shows an 80 % reduction in NO emissions. For CO emissions, both modes maintain CO emissions within 10 ppm/kW, indicating high combustion efficiency. The simulation result shows that a significant increase in the percentage of NNH generated through the reaction of NO and NH_2 in the NO reduction process within the dual flame, leading to a notable reduction in NO_x emissions. In addition, a fraction of NH_2 undergoes thermal decomposition, resulting in the formation of NH, but a portion of this process diminishes as the preheated air temperature rises.

1. Introduction

Driven by the need to reduce carbon emissions and tackle global climate change, ammonia has garnered significant international attention as a carbon-neutral and clean fuel (Luis F. Cardona, 2023). Ammonia is regarded as an excellent hydrogen storage medium due to its lower liquefaction difficulty, ease of storage, and transportation, hence overcoming the challenges associated with hydrogen storage and transportation (Kurien and Mittal, 2022). Furthermore, the advantage of ammonia combustion lies in its production of solely water and nitrogen as byproducts (Alnajideen et al., 2024), effectively avoiding carbon emissions (Chehade et al., 2021). However, despite the potential of ammonia in the energy sector, its application still faces two main challenges: reducing nitrogen oxide (NO_x) emissions and achieving stable combustion (Alnasif et al., 2022). Okafor et al. (2021) investigated swirl combustion of liquid ammonia in preheated air at 500 K and liquid ammonia/methane mixture combustion. The results revealed that mixed combustion enhanced flame stability, reduced flame height, and improved combustion efficiency, with the optimal stable equivalence ratio ranging from 0.66 to 1.37. Achieving low NO_x emissions remains a critical issue, prompting many researchers to actively engage in related studies. Valera-Medina et al. (2017) conducted simulations to compare five different ammonia/methane reaction mechanisms applicable to gas turbines, showing that increasing the inlet temperature of the combustion chamber under high-pressure conditions leads to increased NO_x emissions.

Paper Received: 8 May 2024; Revised: 26 July 2024; Accepted: 4 November 2024
Please cite this article as: Wang S., Chong C.T., Chiong M.-C., 2024, Effect of Air Preheating on the NOx Emissions and Reaction Kinetics of Ammonia/Methane Flames under Different Fuel Injection Strategies, Chemical Engineering Transactions, 113, 175-180 DOI:10.3303/CET24113030

Numerical simulations have been utilised to examine the NO_x emissions mechanism. High fidelity numerical simulations contribute to a deeper understanding of the complex interactions between turbulence and chemical reactions during ammonia combustion, which enhance comprehension of combustion mechanisms. Li et al. (2016) showed that under preheating conditions, the presence of ammonia in air leads to an increase in NO during lean combustion, with NO levels rising with increasing temperature. Conversely, under rich combustion conditions, NO emission decreases. The study demonstrates the significant impact of NH_3 preheating combustion on the formation and decomposition of NO. Additionally, due to the low reactivity and slow combustion rate of ammonia, increasing the inlet temperature can significantly enhance ammonia combustion efficiency and more accurately simulate typical gas turbine operating conditions.
The present study examines the influence of air preheating on NO_x emissions for ammonia-methane flame combust under fully premixed and dual-flame modes. The flame structure of the flames are compared, while the pollutant emissions were measured. Numerical simulation is performed via the chemical reaction network model to analyse the NO formation sensitivity under different preheated air temperatures.

2. Measurement techniques

2.1 Swirl flame burner system

The swirl burner used in this experiment consists of a quartz combustion chamber and a 304 stainless steel swirler. The dimensions of the quartz window are 80 × 80 × 200 mm, and the swirler is equipped with eight straight guide vanes set at a 45-degree angle. The swirler is positioned at the outlet of the burner. The geometric swirl number (S_N) of the burner is calculated by Eq(1):

$$S_N = \frac{2}{3}\left[\frac{1-(D_h/D_s)^3}{1-(D_h/D_s)^2}\right] \times \tan\theta \quad (1)$$

where D_h is the hub diameter, D_s represents the diameter at the tip of the swirler, and θ is the angle between the swirl vanes and the centerline. The calculated S_N is 0.79, which is sufficient to generate a high swirl intensity (S_N > 0.6), achieving flame stabilization through central and outer recirculation zones and forming a V-shaped flame (Mansour et al., 2008). For the dual flame, the pilot flame has a significant impact on the central recirculation zone (CRZ). Previous studies have shown that the introduction of NH_3 through the pilot jet flame in dual-fuel operation significantly affects the CRZ. The overall S_N reduces to 0.21, indicating a substantial alteration in the flow structure (Wang et al., 2023).
Figure 1 depicts the swirl flame burner and the fuel delivery systems for two injection strategies. In the dual-fuel dual swirl flame setup, CH_4 and air are premixed in the plenum, while NH_3 is premixed separately in the central tube. This generates two interacting flames. The burner can also operate in a fully premixed swirl flame mode,

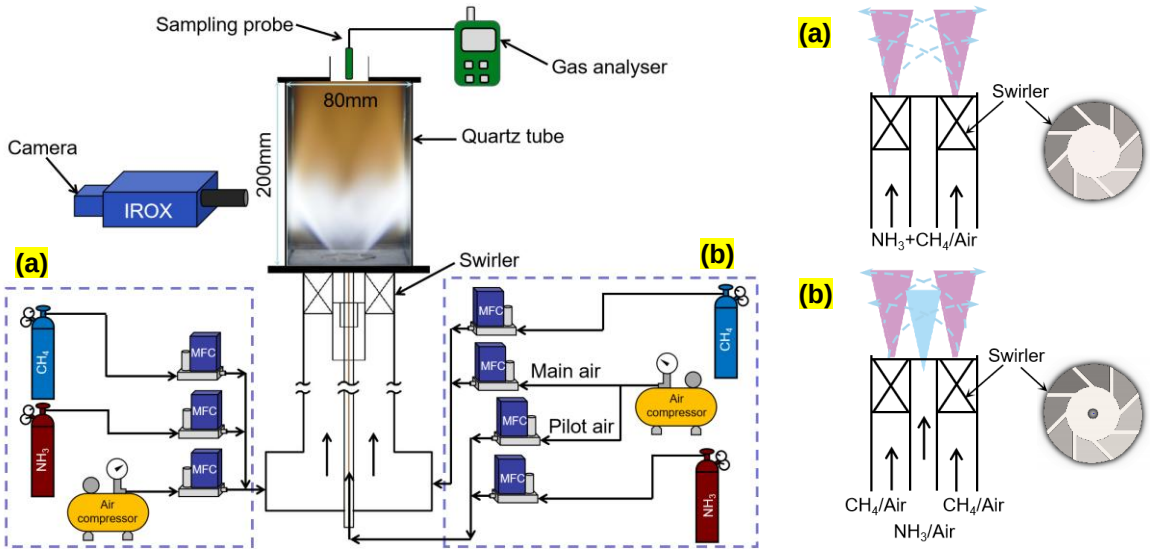

Figure 1: Schematic diagram of (a) premixed and (b) dual-fuel ammonia-methane injection strategy and measurement techniques in swirl flame combustion system.

where NH_3, CH_4, and air are mixed in the plenum before reaching the burner outlet. The use of mass flow controllers enables constant flow of gaseous fuel and air flow, with an accuracy of ±1.0 % of the full scale. The

primary airflow is preheated to 473 K using a 0.55 kW in-line air heater with a PID controller. A K-type thermocouple positioned 30 mm below the burner outlet provides temperature feedback to the controller. Both the burner and preheating pipeline are insulated with high-temperature ceramic wool to minimise heat loss.

2.2 Flame imaging and emissions analysis

The flame chemiluminescence of excited OH* species was captured using a LaVision Imager SX 4M CCD camera with an IRO X image intensifier and an 85 mm Nikon lens. The camera, with a resolution of 2360×1776 pixels, operated at 30 Hz with an 8 ms exposure time. A 308 nm±5 nm filter was used for OH^* detection. For each flame, 150 images were averaged. Abel inversion was then applied to obtain the planar distribution of chemiluminescence signals. The measurement of emissions after combustion was carried out using a KANE 9206 Quintox gas analyser to determine the distribution of NO, NO_2, CO. To facilitate the collection and measurement of the flue gases produced by the rotating flame, a stainless steel cylinder with dimensions of 80×80×350 mm was installed at the flame outlet to serve as a combustion chamber. The extended flame tube was exposed to the atmosphere, but the outlet size was reduced to 50 mm to allow for single-point sampling once the flame had stabilised. Gas sampling was conducted through a 5 mm diameter inlet at a rate of 2 L/min. Each test lasted for 180 seconds to ensure the stability of the readings. The uncertainties are ±5 % for NO, ±5 ppm for NO_2, and ±5 % for CO. High-resolution actual flame images capturing the overall flame were obtained using a Sony A35 digital single-lens reflex (DSLR) camera with an exposure time of 1/320 second.

2.3 Operating conditions

Table 1 presents the operating conditions for the experimental setup of premixed flames and dual-fuel flames established under atmospheric conditions. For the emission measurements, a 20/80 v/v NH3/CH4 mixture was selected to establish a stable flame, enabling measurements over a wider range of equivalence ratios, particularly in the fuel-lean region. Method to determine the air-fuel ratio is shown in previous publication (Wang et al., 2023). To investigate the effect of preheated air on flame structure and emissions, the primary swirling air was preheated to 373 K, 423 K, and 473 K.

Table 1: Experimental conditions for NH_3/CH_4 premixed/dual flames at 298K/373K/423K/473K.

NH_3:CH_4 （v/vol%）	Main swirl air mass flow rate (g/ s)	Methane mass flow rate (g/s)	Pilot air mass flow rate (g/s)	Ammonia mass flow rate (g/s)	Globalϕ	Power (kW)
Premixed						
20/80	2.586	0.073	/	0.019	0.53	4.01
20/80	2.586	0.077	/	0.020	0.56	4.22
20/80	2.586	0.083	/	0.022	0.60	4.58
20/80	2.586	0.090	/	0.024	0.65	4.93
Dual flame						
20/80	2.155	0.077	0.431	0.020	0.56	4.22
20/80	2.155	0.083	0.431	0.022	0.60	4.58
20/80	2.155	0.090	0.431	0.024	0.65	4.93
20/80	2.155	0.096	0.431	0.026	0.70	5.28
20/80	2.155	0.103	0.431	0.027	0.74	5.60

2.4 Numerical simulation

To investigate the chemical reaction mechanism, a chemical reactor network (CRN) model within ANSYS Chemkin-Pro is employed to simulate the swirl flames. The CRN model consists of a combination of perfectly stirred reactor and plug flow reactor (PSR-PFR) models to simulate the fluid dynamics and mixing characteristics within a swirl combustor. The modeling of the premixing section is performed using four perfectly stirred reactors (PSRs), and the recirculation zone is divided into an external recirculation zone (ERZ) and a CRZ. Additionally, the model incorporates a single plug flow reactor (PFR) of 80 mm length to simulate the premixing section. The intensity of the PFR cycle is set to 70 % of the product gas, with the ERZ set to 5 % and the CRZ set to 25 % (Mashruk et al., 2022). In this study, numerical simulations were conducted under specified initial pressure and temperature conditions, using adiabatic conditions to simulate the absence of heat loss to the environment. The model incorporates the comprehensive reaction mechanism developed by Okafor et al. (2018), which includes 59 chemical species and 356 reactions. This study focuses on the NO formation mechanism, using a 20/80 v/v NH_3/CH_4 mixture to investigate NO sensitivity and NH_3 reaction pathways under the influence of preheated air. The fuel mixture and oxidiser are supplied to the reactor network at various initial temperatures, ranging from 298 K to 473 K, consistent with the experimental conditions. The model calculates the average residence time based on empirical flow data, specifying the residence time as 0.5 ms for each configuration.

3. Results and Discussion

Figure 2 illustrates the flame images in the first row and Abel-transformed OH^* chemiluminescence images in the second row for premixed and dual flames of NH_3/CH_4 (20/80 vol.%), at a global equivalence ratio (ϕ) of 0.6 and preheat air temperatures of 298 K and 473 K. Overall, the premixed flames exhibit pale blue flame roots due to the lean mixture at ϕ= 0.6. As the preheated air temperature increases, the intensity of OH^* increases due to the elevated reaction zone temperature, while the overall flame structure remains similar. The difference between the premixed flame and dual-flame is clearly evident, in which the former exhibits a bluish flame zone with V-shape flame brush, whereas the dual-flame model exhibits an elongated luminous NH_3 jet flame at the center, surrounded by a compact faint bluish V-shaped CH_4 swirl flame. This results in distinct combustion zones and varying chemical reactions, thus influencing the flame structure and emission characteristics.
In general, the chemiluminescence signal of OH^* is primarily influenced by the flame temperature and global equivalence ratio. From Figures 2a and b, it can be observed that for premixed combustion, the strongest OH^* signal is located at the base of the V-shaped flame, stabilised by the CRZ and ERZ. The chemiluminescence intensity of OH^* increases with increasing preheat air temperature.

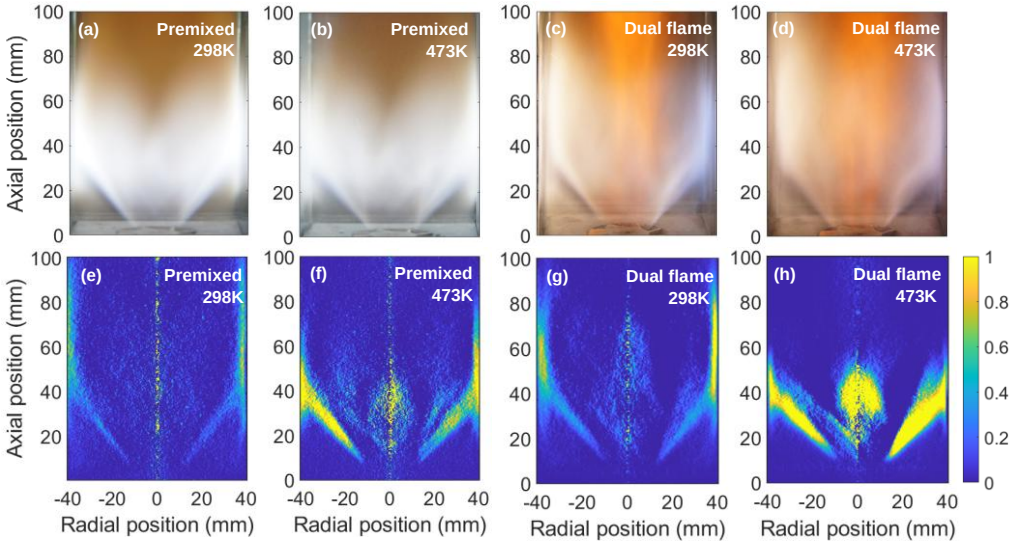

Figure 2: Global flame images (first row) and Abel-transformed OH^* chemiluminescence images (second row) for premixed and dual flames of NH_3/CH_4 (20/80 vol.%) at ϕ_g = 0.6 and temperatures of 298 K and 473 K.

Figure 3 compares the NO, NO_2, and CO emissions of globally lean (ϕ=0.53~0.74) NH_3/CH_4 20/80 vol.% flames at different primary air preheating temperatures, showing that NO emissions increase with preheating for premixed flames but decrease significantly for dual flames at 373 K, especially at ϕ=0.56, 0.65 and 0.7. In premixed flames, the increase in NO emissions is primarily attributed to the enhanced reduction reactions of NH_2 and NH radicals, which subsequently augment NO formation (Mashruk et al., 2022). Comparing fully premixed combustion with dual flame combustion modes at T=473 K and ϕ= 0.6, the latter demonstrates an 80% reduction in NO emissions. The reactions $NH_2 + HO_2 \leftrightarrow NH_3 + O_2$ and $NH_2 + HO_2 \leftrightarrow HNO + H_2O$ are dominant in the pathways leading to NH_3 and NO formation, while the reaction $NH_2 + NH_2 \leftrightarrow NH + NH_3$ significantly contributes to the formation of NH_3 and NH. Similarly, for premixed flames, NO_2 emissions increase with preheating, but for dual flames, the emissions stabilise from 298K to 423K with a slight decrease, and at 473K, NO_2 is almost completely consumed, indicating its role as an intermediate species. For CO emissions, an increase in the equivalence ratio corresponds to a gradual decrease in CO, with dual flame modes consistently showing lower CO emissions. Both flame types maintain CO emissions to within 10 ppm/kW, indicating high combustion efficiency. Above ϕ= 0.6, CO emissions show minimal variation regardless of the preheat temperature, with only slight fluctuation observed. The preheating of primary air increases NO formation as the temperature rises from 298 K to 473 K. This is due to enhanced chemical reaction rates, intensifying the flame and affecting both NO generation and consumption. Under high-temperature conditions, reactions such as $N + OH \leftrightarrow NO + H$, $N + O_2 \leftrightarrow NO + O$, and $N_2 + O \leftrightarrow N + NO$ led to higher thermal NO formation, as shown by Viswamithra et al. (2023) in their study on NH_3/CH_4/air swirl combustion.

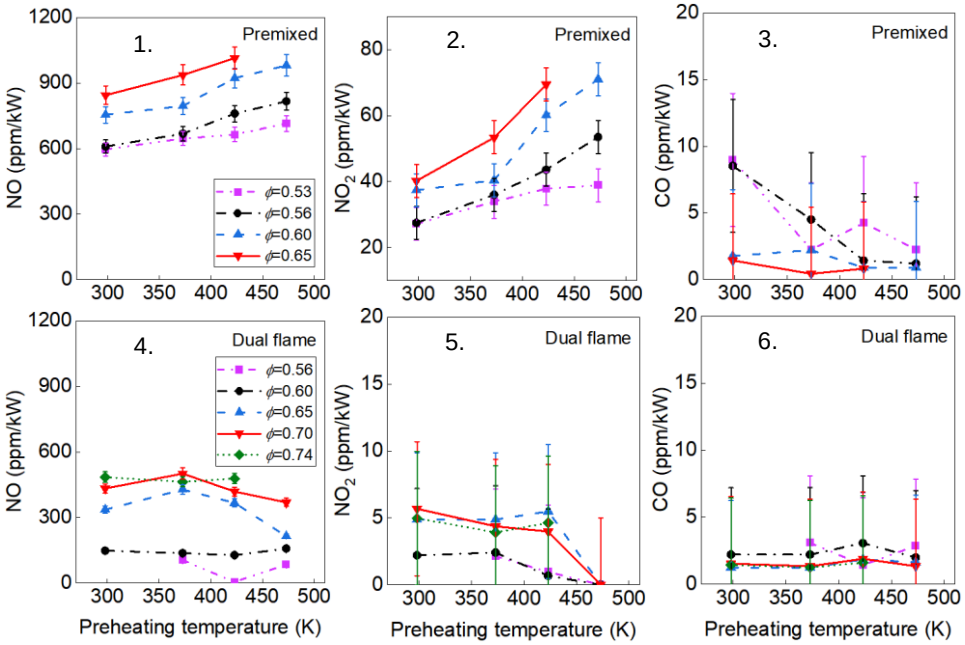

Figure 3: Emissions of NO, NO_2, CO for premixed and dual flames of NH_3/CH_4 20/80 vol.% established at various main swirl air preheat temperatures and equivalence ratio.

Figure 4 shows the normalised sensitivity coefficients of NO for NH_3/CH_4 20/80 vol.% flames under premixed and dual-flame modes at ϕ=0.6 and various main air preheating temperatures derived from CRN modelling. The reaction $NH_2 + O \leftrightarrow HNO + H$ positively influences both flame types by enhancing NH_2 consumption and HNO generation. In premixed flames, $N_2O + O \leftrightarrow 2NO$ and $NH + O \leftrightarrow NO + H$ significantly impact NO formation, while in dual flames, $H + O_2 \leftrightarrow O + OH$ and $NH_2 + O \leftrightarrow HNO + H$ have a greater influence. The key reactions for NO decomposition in premixed flames are $NH + NO \leftrightarrow N_2O + H$, $NO + O + M \leftrightarrow NO_2 + M$, and $NH_2 + NO \leftrightarrow NNH + OH$. For dual flames, the key reactions are $NH_2 + NO \leftrightarrow N_2 + H_2O$, $NH + NO \leftrightarrow N_2O + H$ and $NH_2 + NO \leftrightarrow NNH + OH$. Both flame types consider $NH_2 + NO \leftrightarrow NNH + OH$ crucial for the formation of NNH and OH species. $NH_2 + NO \leftrightarrow N_2 + H_2O$ shows a negative sensitivity in dual flames, indicating that increased reaction rates favor N_2 and H_2O production from NH_2 and NO over NO consumption. It is worth noting that the $NH_2 + NO \leftrightarrow NNH + OH$ reaction has a significant impact on the reduction of NO in dual flames. Specifically, this reaction

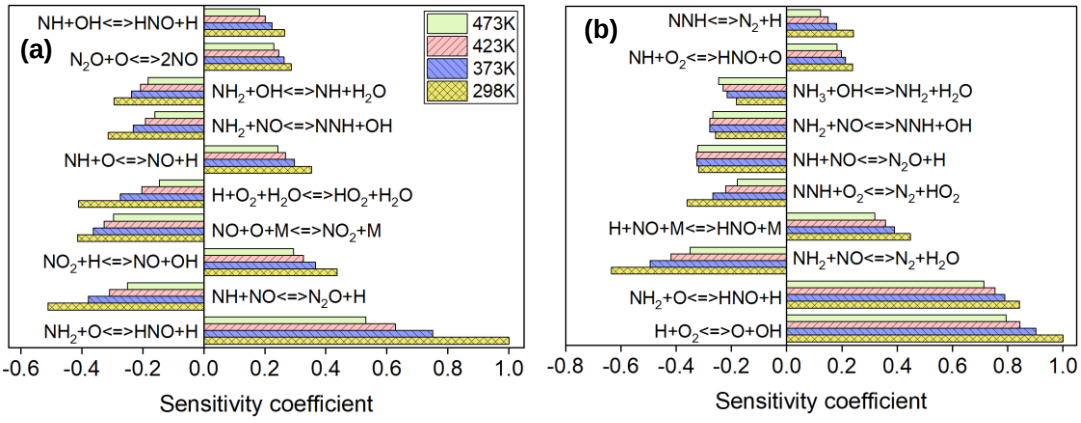

Figure 4: Analysis of NO sensitivity coefficients for NH_3/CH_4 20/80 vol.% flames established at different main air preheating temperatures, ϕ= 0.6, under (a) premixed and (b) dual flame modes.

is enhanced as the preheat temperature of the primary air increases. This is mainly attributed to the additional NH_2 radicals produced from the decomposition of residual NH_3, indicating a pathway for NO suppression during the combustion of NH_3. Furthermore, this trend contrasts with the behavior observed in fully premixed flames.

4. Conclusions

This study primarily compared the effects of preheated air temperature on NO emissions in dual flames and premixed flames. Through flame imaging, pollutant emission measurements, and numerical simulation analysis, an insight was achieved with regards to the effect of preheating and lower NO emissions in dual flames compared to premixed flames. The main conclusions are as follows:

1. The OH* intensity rises with increasing preheated air temperatures, leading to increased NO formation as the air temperature rises from 298 K to 473 K due to enhanced chemical reaction rate, which affects both the formation and consumption rates of NO. The relevant reactions include $N + OH \leftrightarrow NO + H$, $N + O_2 \leftrightarrow NO + O$, and $N_2 + O \leftrightarrow N + NO$.

2. NO emissions increase with primary air preheating in premixed flames but decrease significantly in dual flames at 373 K, particularly at equivalence ratios ϕ=0.56, 0.65, and 0.7. The increase in NO emissions with preheating in premixed flames is primarily due to enhanced reduction reactions of NH_2 and NH radicals, which augment NO formation. The reactions $NH_2 + HO_2 \leftrightarrow NH_3 + O_2$ and $NH_2 + HO_2 \leftrightarrow HNO + H_2O$ are dominant in the pathways leading to NH_3 and NO formation, while the reaction $NH_2 + NH_2 \leftrightarrow NH + NH_3$ significantly contributes to the formation of NH_3 and NH.

3. Dual flame combustion modes exhibit an 80% reduction in NO emissions compared to fully premixed combustion at T=473 K and ϕ=0.6, indicating the potential of NO emissions reduction. Both fully premixed and dual flame combustion modes maintain CO emissions to within 10 ppm/kW.

Acknowledgments

The funding from the Science and Technology Commission of Shanghai Municipality (23160712400) is gratefully acknowledged.

References

Alnajideen, M., Shi, H., Northrop, W., Emberson, D., Kane, S., Czyzewski, P., Alnaeli, M., Mashruk, S., Rouwenhorst, K., Yu, C., Eckart, S., Valera-Medina, A. 2024. Ammonia combustion and emissions in practical applications: a review. Carbon Neutrality, 3(1), 13.

Alnasif, A., Mashruk, S., Kovaleva, M., Wang, P., Valera-Medina, A. 2022. Experimental and numerical analyses of nitrogen oxides formation in a high ammonia-low hydrogen blend using a tangential swirl burner. Carbon Neutrality, 1(1), 24.

Chehade, G., Dincer, I. 2021. Progress in green ammonia production as potential carbon-free fuel. Fuel, 299, 120845.

Kurien, C., Mittal, M. 2022. Review on the production and utilization of green ammonia as an alternate fuel in dual-fuel compression ignition engines. Energy Conversion and Management, 251, 114990.

Li, J., Huang, H., Yuan, H., Zeng, T., Yagami, M., Kobayashi, N. 2016. Modelling of ammonia combustion characteristics at preheating combustion: NO formation analysis. International Journal of Global Warming, 10(1-3), 230-241.

Luis F. Cardona., P. N. A. 2023. Numerical study of MILD Combustion of Ammonia/hydroge Mixtures. Chemical Engineering Transactions, 98.

Mansour, M., Chen, Y.-C. 2008. Stability characteristics and flame structure of low swirl burner. Experimental Thermal and Fluid Science, 32(7), 1390-1395.

Mashruk, S., Kovaleva, M., Alnasif, A., Chong, C. T., Hayakawa, A., Okafor, E. C., Valera-Medina, A. 2022. Nitrogen oxide emissions analyses in ammonia/hydrogen/air premixed swirling flames. Energy, 260, 125183.

Okafor, E. C., Naito, Y., Colson, S., Ichikawa, A., Kudo, T., Hayakawa, A., Kobayashi, H. 2018. Experimental and numerical study of the laminar burning velocity of CH4–NH3–air premixed flames. Combustion and Flame, 187, 185-198.

Okafor, E. C., Yamashita, H., Hayakawa, A., Somarathne, K. D. K. A., Kudo, T., Tsujimura, T., Uchida, M., Ito, S., Kobayashi, H. 2021. Flame stability and emissions characteristics of liquid ammonia spray co-fired with methane in a single stage swirl combustor. Fuel, 287, 119433.

Valera-Medina, A., Xiao, H., Marsh, R., Bowen, P. 2017. Numerical study assessing various ammonia/methane reaction models for use under gas turbine conditions. Fuel, 196, 344-351.

Viswamithra, V., Gurunadhan, M., Menon, S. 2023. Expanding swirl combustor operability on methane-ammonia-air mixtures using a distributed fuel injection technique and inlet air preheating. International Journal of Hydrogen Energy, 48(3), 1189-1201.

Wang, S., Chong, C. T., Xie, T., Józsa, V., Ng, J.-H. 2023. Ammonia/methane dual-fuel injection and Co-firing strategy in a swirl flame combustor for pollutant emissions control. Energy, 281, 128221.